PERGAMON

International Journal of Solids and Structures 40 (2003) 3955–3966

INTERNATIONAL JOURNAL OF SOLIDS and STRUCTURES

www.elsevier.com/locate/ijsolstr

Buckling optimization of plates with variable thickness subjected to nonuniform uncertain loads

A.R. de Faria, S.F.M. de Almeida *

Instituto Tecnológico de Aeronáutica, ITA-CTA-IEM, São José dos Campos, SP 12228-901, Brazil

Received 30 July 2002; received in revised form 26 March 2003

Abstract

The problem of optimizing buckling loads of plates with variable thickness is addressed within the scope of a novel approach where the variability or uncertainty of the loading distribution is taken into account. The loading distribution is not uniform as traditionally assumed but is of a linear piecewise nature otherwise arbitrary. The importance of this investigation lies in the fact that the actual loading distributions acting upon structural components are rarely perfectly uniform although they are usually treated as so in traditional design approaches. A min–max strategy is used to handle the loading variability such that the resulting optimal design is able to withstand an entire class of linear piecewise loadings.

Keywords: Variable thickness plate; Optimization; Nonuniform loads

1. Introduction

Buckling optimization of composite aerospace structural components is an issue of utmost importance. It leads to lighter, more reliable structures that can operate under extreme conditions in hostile environments (e.g. high altitudes, high/low temperatures).

A number of investigations have been conducted in the past addressing the topic (Chao et al., 1975; Hirano, 1979; Haftka and Walsh, 1992; Foldager, 1999; Miki and Sugiyama, 1993). Different strategies and assumptions have been adopted to optimize isotropic and composite plates against buckling. Design variables such as number of plies, ply thickness, continuous ply orientation, discrete ply orientation, reinforcement height and position, and lamination parameters were considered in order to obtain optimal designs. However, in most investigations, the distribution of the applied loads remains fixed and uniform such that the load magnitude is maximized. For instance, it is usual to assume that a known fixed load ratio exists between the normal loads along each axis, when plates under biaxial loads are studied. Moreover, both loading distributions are usually uniform.

* Corresponding author. Fax: +55-12-394-75967.
E-mail address: frascino@mec.ita.br (S.F.M. de Almeida).

0020-7683/03/$ - see front matter
doi:10.1016/S0020-7683(03)00177-X

The assumption of specified loading configuration may result in optimal designs extremely sensitive to variability in the loading. The example of trusses optimized for minimum mass subjected to maximum stress constraints is classic (Vanderplaats, 1984). If there are multiple load cases, optimizing the truss against only one of them may render the structure vulnerable to the others.

In the case of buckling optimization the traditional approach is to assume a uniform loading distribution and maximize its magnitude (Sun and Hansen, 1988). In the design and analysis of aeronautical structural components, tables and diagrams are available in the literature (Bruhn, 1973) and are still widely used by aircraft manufacturers. These tables and diagrams deal almost exclusively with the uniform loading situation. Nevertheless, it is highly unlikely that a perfectly uniform loading is observed in practical applications. Quite frequently, ribs, skin panels or control surfaces are subjected to compressive loadings applied along its edges that are nonuniformly distributed. Moreover, since hundreds of load cases may exist, the loading distribution is nonuniform and may significantly vary during operation.

In this scenario, it is expected that optimal designs obtained under the assumption of uniform loading will perform poorly when another loading distribution is applied, i.e., the optimal design is highly sensitive to loading variations. The fundamental idea of this paper is to tackle the problem of optimal buckling loads whenever the loading distribution is arbitrarily piecewise linear. The loading distributions belong, therefore, to a class of loadings but are otherwise uncertain or not fixed.

Cherkaev and Cherkaeva (1999) were concerned with the sensitivity of optimal minimum compliance designs to perturbations in the distributed applied loads. They proposed a min–max strategy to reduce the high sensitivity observed. A similar technique is used in the present approach where the loading distributions vary during the optimization search such that the resulting optimal design is the one obtained for the worst possible loading configuration. This technique resembles a worst case type analysis or an anti-optimization problem (Bem-Haim and Elishakoff, 1990). A thorough discussion of the technique is not the focus of this work. Only a brief explanation is presented but its rigorous proof and application to several buckling optimization problems is well documented and the interested reader can consult a number of references (de Faria and Hansen, 2001a,b).

The general linear piecewise loading distribution is represented through a series of linear piecewise functions defined at specific locations along the plate edges. It must be emphasized that the refinement of the loading representation and the FE mesh are independent although some degree of relationship is desirable to keep numerical procedures as simple as possible. The more linear piecewise functions are used, the broader the class of admissible loadings. Obviously, the uniform loading distribution can be obtained by a suitable choice of the basis linear piecewise functions.

2. Problem formulation

The design variables of the optimization problem considered are the plate thickness and load distributions that vary continuously while the objective function is the critical buckling load. Calculation of the objective function is based on a classical linear prebuckling state and a linearized buckling problem. Furthermore, the plate must be symmetric with respect to its mid-surface, free of initial imperfections and it is simply supported along all edges.

The strips in Fig. 1a represent regions that have different thicknesses. Those regions are referred to as reinforcements due to its discrete nature. An arbitrary linear piecewise loading distribution is also shown in Fig. 1a. A base plate is defined such that the plate thickness at any point cannot be smaller than the thickness of the base plate. Fig. 1b shows an arbitrary cross-section of the plate depicted in Fig. 1a where the thickness of the reinforcements is exaggerated to facilitate visualization. It can be seen that the reinforcements may have different thicknesses and the base plate is shown at the center of the overall plate.

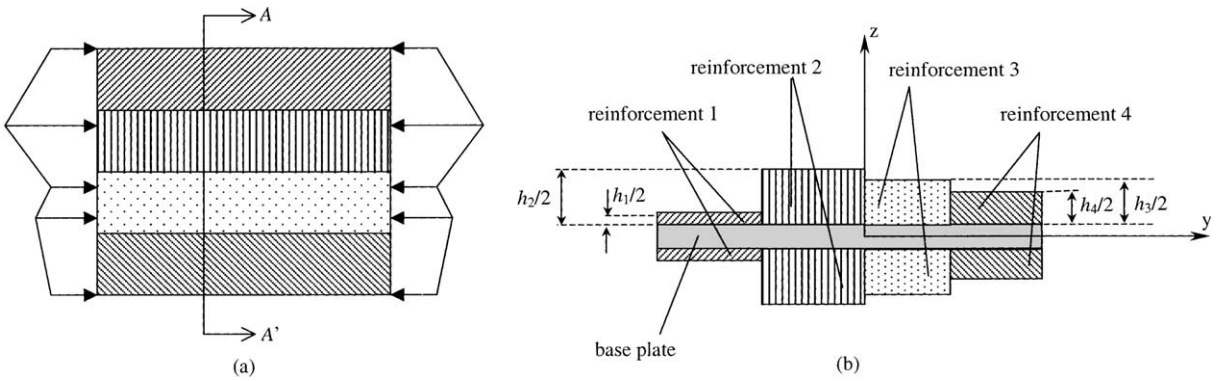

Fig. 1. Variable thickness plate.

Fig. 2a shows one edge of the plate and an arbitrary linear piecewise loading applied. The four points, 1, 2, 3 and 4, are the locations where the basis linear piecewise functions shown in Fig. 2b are defined. A suitable choice of f_1, f_2, f_3 and f_4 (the heights of the triangles in Fig. 2b), represents the loading in Fig. 2a. Notice that points 1, 2, 3 and 4 may not coincide with nodes of the FE mesh as depicted in Fig. 1a but, in order to facilitate numerical procedures, it is desirable to enforce coincidence as illustrated in Fig. 2a.

The heights of the triangles f_1, f_2, f_3, f_4, are actually the variables that describe the loading distribution. Let us denote the height of triangle i by f_i which is now written as in Eq. (1):

$$f_i = R_i \bar{f}_i \tag{1}$$

where $\bar{f}_i$ is an associated scaling factor and $R_i \in [0,1]$ is the proportionality parameter that provides a measure of the contribution of each piecewise linear function to the applied loading. $\bar{f}_i$ is selected such that the areas of all the triangles in Fig. 2c are equal to some value $\bar{f}L$ as in Eq. (2) where m is the number of basis functions and L is the length of the applicable plate edge.

$$\begin{aligned} \bar{f}_1 &= \frac{2\bar{f}L}{l_{12}} \\ \bar{f}_i &= \frac{2\bar{f}L}{l_{i-1,i} + l_{i,i+1}} \quad \text{for } 1 < i < m \\ \bar{f}_m &= \frac{2\bar{f}L}{l_{m-1,m}} \end{aligned} \tag{2}$$

$\bar{f}_i$ provides, therefore, a normalization to the linear piecewise functions such that the contribution of all of them in terms of net force is equal to $\bar{f}L$, $\bar{f}$ being the equivalent uniformly distributed loading. The relative contribution is given by the proportionality parameters R_i. Moreover, in order to maintain a constant net force $\bar{f}L$ the R_i's hold the relationship given by Eq. (3). Additional discussion on the loading representation will be given in the following section.

$$\sum_{i=1}^{m} R_i = 1 \tag{3}$$

Reissner–Mindlin formulation is adopted to model the plate elastic behavior and von Kàrmàn nonlinear strains are used for the buckling problem. Thus, the in-plane displacements $\tilde{u}(x,y,z) = u(x,y) + z\psi_x(x,y)$ and $\tilde{v}(x,y,z) = v(x,y) + z\psi_y(x,y)$ vary linearly through the plate thickness and the transverse displacement $\tilde{w}(x,y,z) = w(x,y)$ is independent of z. Based on these displacement fields the strain vectors are

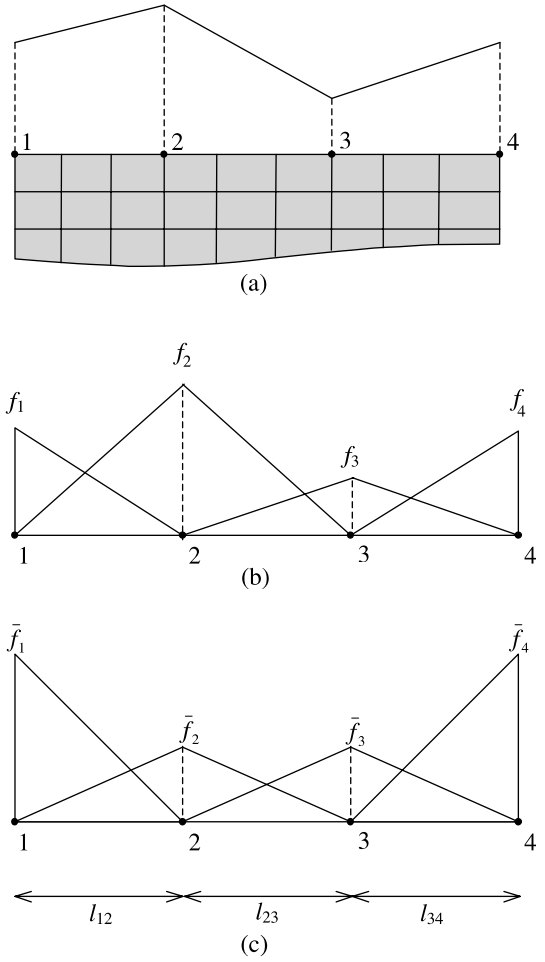

Fig. 2. Discretization of the loading distribution.

$$\boldsymbol{\varepsilon}^{\mathrm{L}}(\mathbf{u}) = \boldsymbol{\varepsilon}^{0} + z\boldsymbol{\kappa} = \begin{Bmatrix} u_{,x} \\ v_{,y} \\ u_{,y} + v_{,x} \end{Bmatrix} + z \begin{Bmatrix} \psi_{x,x} \\ \psi_{y,y} \\ \psi_{x,y} + \psi_{y,x} \end{Bmatrix}$$
$$\boldsymbol{\gamma}^{0}(\mathbf{u}) = \begin{Bmatrix} w_{,x} + \psi_x \\ w_{,y} + \psi_y \end{Bmatrix}, \quad \boldsymbol{\varepsilon}^{\mathrm{N}}(\mathbf{u}) = \frac{1}{2} \begin{Bmatrix} w_{,x}^2 \\ w_{,y}^2 \\ 2w_{,x}w_{,y} \end{Bmatrix} \tag{4}$$

where $\boldsymbol{\varepsilon}^{\mathrm{L}}$ is the linear strain vector, $\boldsymbol{\varepsilon}^{0}$ is the in-plane linear strain vector, $\boldsymbol{\kappa}$ is the vector of curvatures, $\boldsymbol{\gamma}^{0}$ is the vector of out-of-plane shear strains, $\boldsymbol{\varepsilon}^{\mathrm{N}}$ is nonlinear strain vector and $\mathbf{u} = (u, v, w, \psi_x, \psi_y)$. Using the above, the linearized total potential energy is

$$\Pi = \frac{1}{2} \int_{\Omega} \begin{Bmatrix} \boldsymbol{\varepsilon}^{0} \\ \boldsymbol{\kappa} \\ \boldsymbol{\gamma}^{0} \end{Bmatrix}^{\mathrm{T}} \begin{bmatrix} \mathbf{A} & \mathbf{B} & \mathbf{0} \\ \mathbf{B} & \mathbf{D} & \mathbf{0} \\ \mathbf{0} & \mathbf{0} & \mathbf{A}^{*} \end{bmatrix} \begin{Bmatrix} \boldsymbol{\varepsilon}^{0} \\ \boldsymbol{\kappa} \\ \boldsymbol{\gamma}^{0} \end{Bmatrix} \mathrm{d}\Omega - \int_{\Gamma} \mathbf{u}^{\mathrm{T}} \mathbf{t} \, \mathrm{d}\Gamma \tag{5}$$

where $\mathbf{A}$, $\mathbf{B}$, $\mathbf{D}$, $\mathbf{A}^*$ are the laminate stiffness matrices given in Daniel and Ishai (1994), Ω is the plate mid-plane, Γ are the plate mid-plane edges and $\mathbf{t}$ is the vector of forces applied on Γ. The expression for the second variation of the total potential energy (Koiter, 1945) can be written as

$$P_2[\mathbf{u}] = \frac{1}{2}\int_\Omega \begin{Bmatrix} \boldsymbol{\varepsilon}^0 \\ \boldsymbol{\kappa} \\ \boldsymbol{\gamma}^0 \end{Bmatrix}^{\mathrm{T}} \begin{bmatrix} \mathbf{A} & \mathbf{B} & \mathbf{0} \\ \mathbf{B} & \mathbf{D} & \mathbf{0} \\ \mathbf{0} & \mathbf{0} & \mathbf{A}^* \end{bmatrix} \begin{Bmatrix} \boldsymbol{\varepsilon}^0 \\ \boldsymbol{\kappa} \\ \boldsymbol{\gamma}^0 \end{Bmatrix} \mathrm{d}\Omega - \int_\Omega (\boldsymbol{\varepsilon}^{\mathrm{N}})^{\mathrm{T}} \begin{Bmatrix} N_x \\ N_y \\ N_{xy} \end{Bmatrix} \mathrm{d}\Omega \tag{6}$$

where N_x, N_y, N_{xy} are membrane forces resulting from the prebuckling state, Eq. (5). Observe that, in Eq. (6), advantage has been taken of the fact that the laminate is symmetric and in-plane loads are applied to write the second integral. Because of the linearity of the prebuckling problem the forces N_x, N_y, N_{xy} can be written as the product of a proportionality parameter λ and a reference state $\overline{N}_x$, $\overline{N}_y$, $\overline{N}_{xy}$ such that $N_x = \lambda\overline{N}_x$, $N_y = \lambda\overline{N}_y$ and $N_{xy} = \lambda\overline{N}_{xy}$. Minimization of the functional $P_2[\mathbf{u}]$ in Eq. (6) provides the critical load λ_{cr}. Numerical solution of both prebuckling and buckling problems is carried out through the finite element method where isoparametric bicubic Lagrange elements with 16 nodes are used (de Faria and Hansen, 1999). Symmetry of the optimal buckling modes cannot be anticipated and, therefore, the entire plate is modeled. The resulting prebuckling and buckling problems can be stated in a matrix form as

$$\begin{aligned} &\mathbf{K}\mathbf{q}_{\mathrm{p}} = \mathbf{f} \\ &(\mathbf{K} - \lambda\mathbf{K}_{\mathrm{G}})\mathbf{q} = \mathbf{0} \end{aligned} \tag{7}$$

where $\mathbf{K}$ is the stiffness matrix, $\mathbf{q}_{\mathrm{p}}$ are the prebuckling displacements, $\mathbf{f}$ is the global vector of applied loads, $\mathbf{K}_{\mathrm{G}}$ is the geometric stiffness matrix due to the nonlinear strains and $\mathbf{q}$ is the buckling mode associated with eigenvalue λ.

3. Optimization for piecewise linear loadings

It is assumed that the basic distributed loadings represented by the linear piecewise basis functions shown in Fig. 2c may be applied individually or as a convex linear combination such that Eq. (3) is valid. In the latter case the resulting applied load is the summation of the contributions of the individual basis loadings. In order to better describe individual contributions of the basis loadings it is convenient to introduce the concept of net force component. The resulting net force F_i of loading distribution i is given by

$$F_i = \lambda R_i \bar{f} L \tag{8}$$

where λ is the buckling load magnitude and R_i is the proportionality parameter introduced in the previous section. The parameters R_i describe the distribution pattern of the load while λ characterizes the load magnitude. The optimization strategy devised yields the worst loading distribution in terms of R_i and λ is the least positive eigenvalue obtained in Eq. (7b). $\bar{f}$ is positive but otherwise arbitrary; it is made equal to $1/L$ for the numerical simulations in this work.

The parameters R_i provide a measure of the contribution of each individual basis loading. These are free to vary during the optimization but they must be positive and add up to one as posed in Eq. (3) such that a convex linear combination is characterized and to guarantee that a normalization of the reference state exists.

In addition to the constraint introduced by Eq. (3) another constraint exists to enforce constant plate volume, i.e., the summation of the reinforcement thicknesses shown in Fig. 1b must not be larger than a given value:

$$\sum_{i=1}^{n} h_i \leqslant nh \tag{9}$$

where n is the number of reinforcement strips and nh is the maximum thickness one reinforcement can reach if all the others are zero.

The definition of reference state force components above allows one to formulate an optimization/antioptimization problem as in Eq. (10) (Cherkaev and Cherkaeva, 1999).

$$\max_{\mathbf{h}} \min_{\mathbf{r}} \lambda(\mathbf{h}, \mathbf{r}) \tag{10}$$

where $\mathbf{h}$ is the vector of reinforcement thicknesses and $\mathbf{r}$ is the vector of uncertain loads $\mathbf{r} = (R_1, \ldots, R_m)$ when m loading components are considered. Solution of the problem stated in Eq. (10) provides, simultaneously, the optimal design and the worst loading combination. This is a bilevel optimization problem whose numerical solution is elaborate. However, the fact that λ is obtained through solution of a classic eigenvalue problem allows for a tremendous simplification. Reformulation of Eq. (10) can be done as follows:

$$\max_{\mathbf{h}} \phi(\mathbf{h}), \quad \phi(\mathbf{h}) = \min_{\mathbf{r}} \lambda(\mathbf{h}, \mathbf{r}) \tag{11}$$

where $\phi(\mathbf{h})$ is actually obtained through solution of a minimization problem. Eq. (11) alone does not permit any simplification. However, if the extended stability boundary theorem (de Faria and Hansen, 2001a) is called upon, evaluation of $\phi(\mathbf{h})$ becomes straightforward.

Fig. 3 presents a sketch of the stability boundary surface for a fixed design $\mathbf{h}$ and the reference plane $\sum R_i = 1$ defined in Eq. (3). The axes in Fig. 3 are the net force components λR_i since $\bar{f}L$ is taken equal to unity (see Eq. (8)). The stability boundary shown in Fig. 3 is concave with respect to the origin of the load space and this is no coincidence. Actually, the extension of the stability boundary theorem guarantees that concavity is always observed provided $\mathbf{K}$ is positive-definite and even when $\mathbf{K}_G$ is indefinite. Therefore, minimization of $\lambda(\mathbf{h}, \mathbf{r})$ with respect to $\mathbf{r}$ is easily accomplished since it suffices to evaluate λ at the vertices of

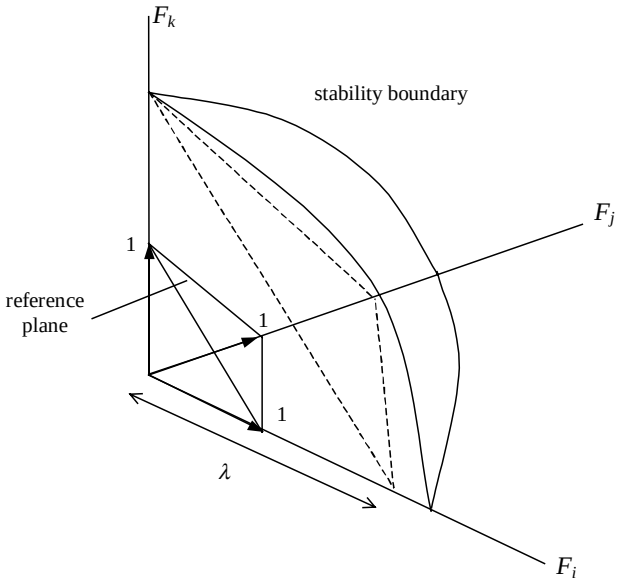

Fig. 3. Stability boundary sketch.

the reference tetrahedron. As λ is increased the reference plane moves away from the origin until it reaches the stability boundary. Furthermore, the theorem guarantees that the point of intersection is necessarily one or more of the vertices given the concavity of the stability boundary.

The bilevel optimization problem stated in Eq. (10) is therefore reduced to a classic optimization problem where the objective function is evaluated by checking the minimum λ associated with the vertices of the reference tetrahedron. The optimization problem is solved in two steps. Firstly, 200 random designs are generated in an attempt to reduce the risk of convergence to local optima. The best design obtained randomly is selected as a starting point for a Powell's search (Powell, 1964). Powell's method is adequate in this case because it is simple and avoids the complications caused by derivatives of possible repeated eigenvalues since gradients of the objective function are not required by the method. The optimization stops when the relative difference between the previous and present values of ϕ does not exceed 0.001.

4. Numerical simulations and discussion

A square plate simply supported along the four edges of 36 cm is investigated with a 0.3 mm thick base plate. The material chosen for simulation is isotropic with Young modulus of 70 GPa and Poisson ratio of 0.30. Four reinforcements are considered and five basis linear piecewise functions are defined at positions $y = 0$, 9, 18, 27 and 36 cm along the two opposite edges parallel to the y-axis. The value of h expressed in Eq. (9) is 0.3 mm and $n = 4$, hence, a reinforcement may have a maximum thickness of 1.2 mm.

In order to establish a comparison between the optimal designs obtained under traditional assumptions of fixed loading configurations and the present strategy it is worth finding a few classic optimal designs. These results are better visualized in a graphical form. Fig. 4a–c present sketches of the optimal plate configurations obtained when specific distributed loading components are applied. The specific loading distributions are assumed to be equal to the considered basis functions $\bar{f}_i$. Fig. 4d presents the optimal plate for the uniform loading. The values within strips are the reinforcement thicknesses. The total thickness is given by the reinforcement thickness plus the base plate thickness. The force magnitudes are the optimal net forces caused by the distributed loadings whose shapes are also shown. Because of the symmetry of the basis functions about $y = 18$ cm, only three cases are shown. Noticeable is the fact that, apart from the uniform loading situation, all of the optimal designs are nonsymmetric with respect to the plate center line $y = 18$ cm, including the case of the distributed load component applied at the center of the plate, Fig. 4c.

Table 1 presents an interesting comparison showing how poorly optimal designs obtained under traditional assumptions can perform in terms of λ when the loading configuration is changed. The lines of Table 1 correspond to the optimal designs presented in Fig. 4a–d and columns correspond to the loading distribution components applied. Notice how bad the same optimal design performs if the loading configuration is changed. For instance, the optimal design of Fig. 4a may have its critical load reduced by a factor of 15 if an unfavorable, unpredicted loading is applied.

Fig. 5 shows the optimal plate obtained by the min–max strategy. As opposed to Fig. 4a–c symmetry with respect to the plate center line $y = 18$ cm is observed. In this case the critical buckling loads are $F_1 = F_5 = 150.4$ N, $F_2 = F_4 = 135.4$ N, $F_3 = 114.9$ N and $F = 151.6$ N for the uniform loading, much less spaced than the results presented in Table 1. For the optimal design presented in Fig. 5 the critical load λ is greater than 114.9 N for any loading combination R_i provided that $\sum R_i = 1$.

Since the stability boundary theorem is the key that allows simplification of the optimization strategy it is interesting to show stability surfaces of the optimal designs obtained (Figs. 4a–d and 5). These are drawn in Fig. 6a–e where the values presented on the axes correspond to λ. It must be emphasized that the problem has five dimensions with respect to the loading. For visualization purposes, only three of them are included in Fig. 6 (F_1, F_2, F_3). As a consequence, Fig. 6 provides interesting views of the stability surfaces but should be examined carefully in order to avoid misleading conclusions as the effect of F_4 and F_5 are not depicted.

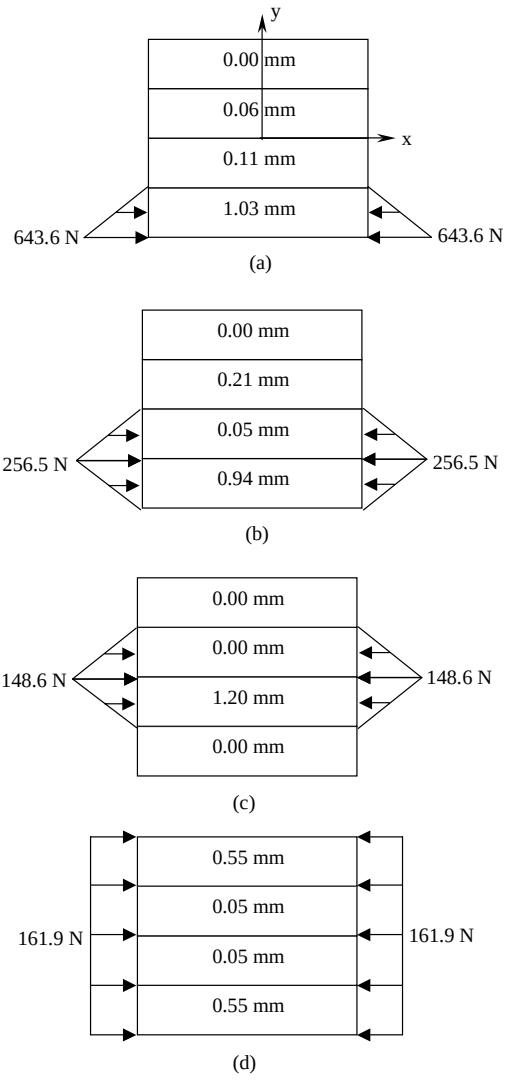

Fig. 4. Classic optimal designs and loads.

The surfaces presented in Fig. 6a, b and d are severely distorted; the magnitudes of F_3 are significantly smaller than those of F_1 and F_2. This means that the structure is very vulnerable to a loading of this type (F_3). In Fig. 6e a much more uniform distribution of buckling loads is seen among the force components. As pointed out, simple comparison of Fig. 6c and e may be misleading because, apparently, the design associated with Fig. 6c is superior. That is not true since the axes F_4 and F_5 are not shown. As soon as axes F_4 and F_5 are considered, the performances of the optimal designs shown in Fig. 6a–d are worse when compared to the performance the optimal design in Fig. 5 obtained by the min–max strategy as can be observed in Table 1.

Fig. 7a–d show the buckling modes associated with the four loading distributions: $R_1 = 1.0$, $R_2 = 1.0$, $R_3 = 1.0$ and $2R_1 = R_2 = R_3 = R_4 = 2R_5 = 0.25$, respectively, for the optimal design presented in Fig. 5. It

Table 1
Sensitivity of traditional optimal designs

Optimization approach	Type of loading					
	$R_1 = 1$	$R_2 = 1$	$R_3 = 1$	$R_4 = 1$	$R_5 = 1$	Uniform
Optimized for $\bar{f}_1$ (Fig. 4a)	643.6	225.6	56.2	37.2	38.7	75.7
Optimized for $\bar{f}_2$ (Fig. 4b)	541.3	256.5	76.6	55.1	47.4	97.4
Optimized for $\bar{f}_3$ (Fig. 4c)	135.4	182.5	148.5	49.3	44.2	114.8
Optimized for uniform loading (Fig. 4d)	208.9	151.2	74.8	151.2	208.9	161.9

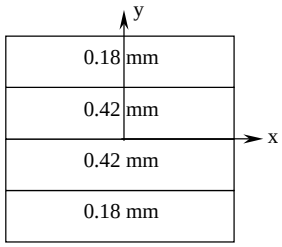

Fig. 5. Optimal design subjected to uncertain loads.

can be seen that different buckling modes are associated with the same optimal design for different force components. That is precisely one of the difficulties that the present strategy helps to overcome: several load cases resulting in different failure modes that must be optimized or eliminated simultaneously.

5. Discussion and conclusions

A novel approach for optimizing structures subjected to different loading distributions is proposed. Advantage is taken from the extended stability boundary theorem in order to expedite the bilevel optimization problem that naturally appears, transforming it into a classic maximization problem with a new objective function that takes into account the multiplicity of loading distributions.

Alternative ways to handle the uncertainty in the loading distributions consist of probabilistic methods. These approaches admit that a given probability density function exists that statistically represents the loading. However, if the probability density function is not known or well defined the results obtained by the optimization methods may be misleading. The present technique avoids working with probability distributions; it provides the optimal extremal properties of the structure (Bem-Haim and Elishakoff, 1990).

The meshes used in all numerical calculations had 16 elements (4×4). Refinement of the plate FE mesh does not significantly alter results since the element used is bicubic Lagragian whose complexity (the element matrix is 80×80) allows for the use of relatively coarse FE meshes. Meshes four times finer (8×8) were tested in all optimal designs presented in Figs. 4a–d and 5 with small variation in terms of buckling loads (<5%).

The conventional approach to practical optimization of real structures consists in selecting one load case deemed to be the most dangerous or commonly used and assume that all the other load cases will not result in failure. This assumption is clearly wrong as can be observed in the simple example investigated in this work. It was determined that the worst loading acting on the optimal plate in Fig. 5 is the one where $R_3 = 1$ which leads to $\lambda = 114.9$ N. Moreover, if the loading configuration is changed, it is guaranteed that

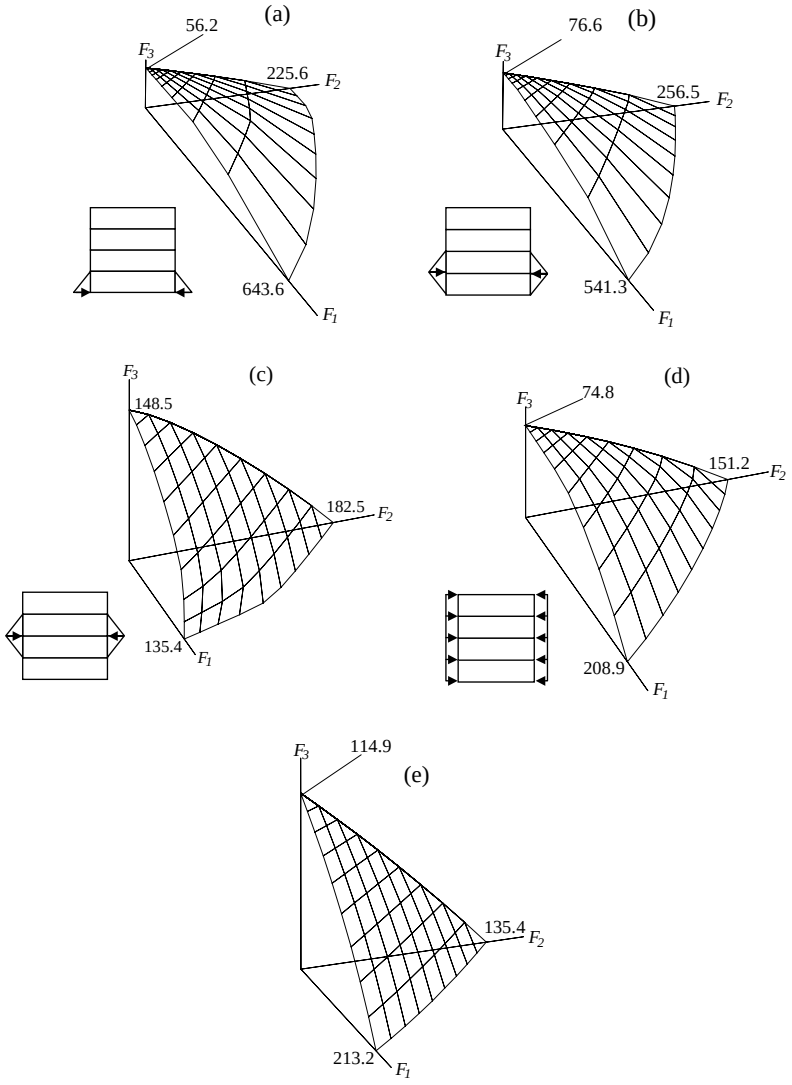

Fig. 6. Optimal stability surfaces.

$\lambda > 114.9$ N. However, when the plate is optimized against $R_3 = 1$ only (Fig. 4c) the loading configuration $R_5 = 1$ leads to $\lambda = 44.2$ N as reported in Table 1. In other words, classic optimal designs may be extremely sensitive to perturbations in the loading configuration.

The uncertain loading distributions considered in this work are associated with one axis of the plate. However, it is possible to consider variations in biaxial loading distributions. The only modification to the present approach would be the inclusion of design variables that relate to the additional components of uncertain loading distributions. The convex combination expressed in Eq. (3) is still observed but now the proportionality parameters R_i relate to either loading along x or y. The strips of variable thickness shown in Fig. 1a may not be the most convenient configuration. Thickness variation in both x and y directions seems to be a more appropriate choice.

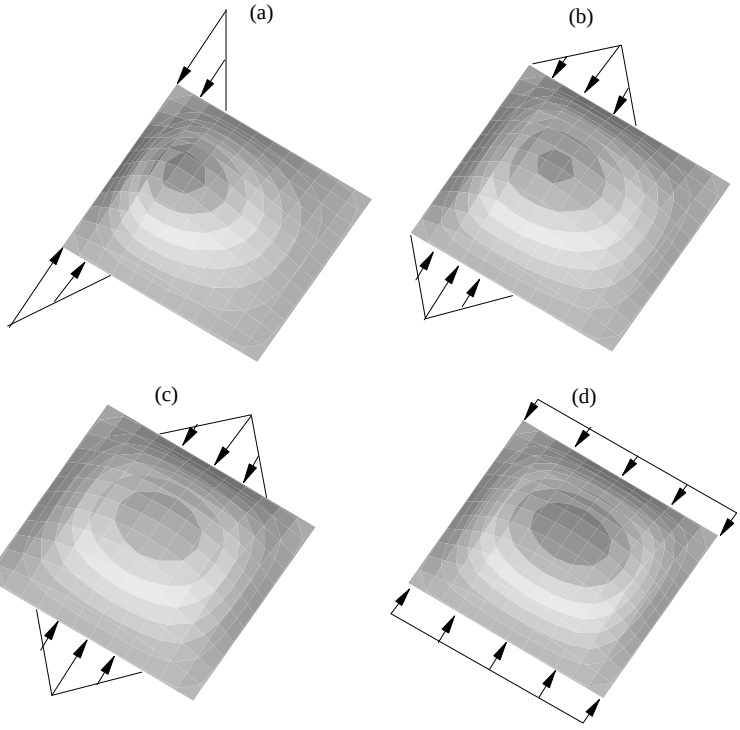

Fig. 7. Buckling modes of optimal design.

Fig. 1a shows that the normal loading distributions on two opposite edges are completely symmetric, i.e., the load is self-equilibrating. Shear loads may not be fully symmetric and still be self-equilibrating as long as the equivalent distributed shear force $\bar{f}$ is the same for all the plate sides. This is a new situation that requires further investigation. If it is assumed that the shear loading distributions on the four sides have are equal shape and the same number of basis functions, then the technique presented can be employed without difficulty just by consideration of additional parameters R_i related to the shear loading.

Eq. (1) implicitly assumes that all the distributed loading components have equal possibility of occurrence since $R_i \in [0, 1]$. However, it may be interesting to favor loadings that are more likely to appear. For instance, the distributed loading may vary but it might be known that a certain percentage of uniform loading is guaranteed to be involved. In this case, Eq. (1) may be reformulated to incorporate this share of certainty by considering fixed percentages of the proportionality parameters such that $R_i = R_{i0} + \Delta R_i$, where R_{i0} is the fixed percentage and ΔR_i the uncertainty portion. The plate simulated in this work has $m = 5$. If it is desirable to specify that 50% of the loading is certainly uniform, then make $2R_{10} = R_{20} = R_{30} = R_{40} = 2R_{50} = 0.125$. Minimization of ϕ in Eq. (11) is slightly different because now the vertices of the convex hull must be checked, not simply the points where the stability surface cross the axis (de Faria and Hansen, 2001a) but there is essentially no modification to the optimization strategy.

The resulting optimal designs obtained by the min–max strategy are insensitive to perturbations in the loading distributions, i.e., if the loading varies within the admissible load set (linear piecewise loadings), it is guaranteed that the buckling load always increases or, in the worst situation, is invariant. The optimal design is the physical realization of a compromise between maximum buckling load and the ability to sustain a variety of loading distributions.

References

Bem-Haim, Y., Elishakoff, I., 1990. Convex Models of Uncertainty in Applied Mechanics. Elsevier Science Publishers, New York.

Bruhn, E.F., 1973. Analysis and Design of Flight Vehicle Structures. Tri-State Offset, Cincinnati, OH.

Chao, C.C., Koh, S.L., Sun, C.T., 1975. Optimization of buckling and yield strengths of laminated composites. AIAA Journal 13 (9), 1131–1132.

Cherkaev, E., Cherkaeva, A., 1999. Optimal design for uncertain loading conditions. In: Berdichevsky, V., Jikov, V., Papanicolaou, G. (Eds.), Homogenization. World Scientific, Singapore, pp. 193–213.

Daniel, I.M., Ishai, O., 1994. Engineering Mechanics of Composite Materials. Oxford University Press, New York.

de Faria, A.R., Hansen, J.S., 1999. Optimal buckling loads of nonuniform composite plates with thermal residual stresses. Journal of Applied Mechanics 66 (2), 388–395.

de Faria, A.R., Hansen, J.S., 2001a. On buckling optimization under uncertain loading combinations. Structural and Multidisciplinary Optimization Journal 21 (4), 272–282.

de Faria, A.R., Hansen, J.S., 2001b. Buckling optimization of composite axisymmetric cylindrical shells under uncertain loading combinations. Journal of Applied Mechanics 68 (4), 632–639.

Foldager, J.P., 1999. Design of composite structures. PhD Dissertation, Aalborg University, Institute of Mechanical Engineering, Special report 39.

Haftka, R.T., Walsh, J.L., 1992. Stacking sequence optimization for buckling of laminated plates by integer programming. AIAA Journal 30 (3), 814–819.

Hirano, Y., 1979. Optimum design of laminated plates under axial compression. AIAA Journal 17 (9), 1017–1019.

Koiter, W.T., 1945. On the stability of elastic equilibrium. PhD Thesis, English translation: Air Force Flight Dynamics Technical Laboratory, Report AFFDL-TR-70-25, February 1970.

Miki, M., Sugiyama, Y., 1993. Optimum design of laminated composite plates using lamination parameters. AIAA Journal 31 (5), 921–922.

Powell, M.J.D., 1964. An efficient method for finding the minimum of a function of several variables without calculating derivatives. Computers Journal 7, 155–162.

Sun, G., Hansen, J.S., 1988. Optimal design of laminated-composite circular–cylindrical shells subjected to combined loads. Journal of Applied Mechanics 55 (3), 136–142.

Vanderplaats, G.N., 1984. Optimization Techniques for Nonlinear Engineering Design with Applications. McGraw-Hill, New York.